
AUTOMATIC MAP UPDATE USING DASHCAM VIDEOS

A PREPRINT

Aziza Zhanabatyrova
Aalto University,
Espoo, Finland,
zhanabatyrova.aziza@aalto.fi

Clayton Souza Leite
Aalto University,
Espoo, Finland,
clayton.souzaleite@aalto.fi

Yu Xiao
Aalto University,
Espoo, Finland,
yu.xiao@aalto.fi

September 28, 2021

ABSTRACT

Autonomous driving requires 3D maps that provide accurate and up-to-date information about semantic landmarks. Due to the wider availability and lower cost of cameras compared with laser scanners, vision-based mapping has attracted much attention from academia and industry. Among the existing solutions, Structure-from-Motion (SfM) technology has proved to be feasible for building 3D maps from crowdsourced data, since it allows unordered images as input. Previous works on SfM have mainly focused on issues related to building 3D point clouds and calculating camera poses, leaving the issues of automatic change detection and localization open.

We propose in this paper an SfM-based solution for automatic map update, with a focus on real-time change detection and localization. Our solution builds on comparison of semantic map data (e.g. types and locations of traffic signs). Through a novel design of the pixel-wise 3D localization algorithm, our system can locate the objects detected from 2D images in a 3D space, utilizing sparse SfM point clouds. Experiments with dashcam videos collected from two urban areas prove that the system is able to locate visible traffic signs in front along the driving direction with a median distance error of 1.52 meters. Moreover, it can detect up to 80% of the changes with a median distance error of 2.21 meters. The result analysis also shows the potential of significantly improving the system performance in the future by increasing the accuracy of the background technology in use, including in particular the object detection and point cloud geo-registration algorithms.

Keywords Mapping, localization, change detection, structure from motion.

1 Introduction

Autonomous driving requires high-definition (HD) 3D maps for safe maneuvering in complex urban environments. Several mapping and self-driving companies such as HERE and TOMTOM have already started to build and consume HD maps. The existing HD maps are mainly created by scanning the environment using high-precision LiDAR sensors. Due to the high costs of LiDAR sensors, only a few vehicles would be equipped with such sensors and scheduled to go through different areas to collect data. This makes it challenging to keep the maps up to date, especially when there is no efficient way to detect and locate changes in the environment.

Compared with LiDAR sensors, visual sensors such as dashcams are much cheaper and have been widely installed on vehicles. Previous works [4][20] have also proved the feasibility of creating accurate 3D point clouds from unordered images using structure from motion (SfM) techniques, which allows the input to be collected through crowdsourcing. Due to the high computational complexity of SfM-based point cloud generation, it is not feasible to reconstruct point clouds whenever new images arrive. Therefore, it becomes essential to effectively detect and localize changes in the environment, and remap only the regions where the changes occurred.

In this paper, we extend the previous works [20] on SfM-based mapping and localization to support automatic generation and maintenance of a four-layer map using dashcam video. Our focus is placed on solving the challenges related to automatic extraction of semantic map data with minimal human supervision and manual labeling, as well as real-time change detection and localization in complex urban environments.

Our system advances the state-of-the-art with the following distinguished features. Firstly, it combines image-based semantic segmentation and object detection with SfM to enable accurate point cloud segmentation and further the automatic generation of semantic map data (e.g. types and 3D locations of traffic signs). Secondly, it provides a novel method for utilizing SfM-based point clouds to train a deep learning model for online pixel-wise 3D localization from monocular RGB data. This method allows localizing traffic signs online with respect to the camera poses in a world coordinates system. Compared with our method, previous works either provide only depth information, neglecting the lateral and height information which is necessary for 3D localization, or require heavy manual labeling for training of 3D models. Thirdly, our system supports light-weight change detection by comparing the semantic map data. With the multi-layer design, the dynamic map data representing temporary changes is stored on separate layers.

We collected dashcam video from two urban areas in February and December, 2019, and used the data for evaluating the system performance. The results show that the median distance error of localized traffic signs by the offline localization is 7.72 meters with standard deviation of 5.16. Regarding online change detection, 80% changes are detected with an average distance error of 9 meters.

The rest of the paper is organized as follows. Section 2 reviews the background technology used for building our solution. In Section 3 we give an overview of the system architecture, followed by the designs of the offline and online processes described in Section 4 and Section 5, respectively. The evaluation of these designs using the datasets presented in Section 6 are discussed in Sections 7 and 8, respectively. The related works are summarized in Section 9 before we conclude the paper in Section 11.

2 Background

Structure from motion (SfM). We apply SfM for creating 3D point clouds from 2D images. A typical SfM pipeline consists of 3 steps: feature extraction, feature matching, and bundle adjustment. The first step extracts from images highly distinctive and invariant features, and the second step tries to match features between image pairs. The matches are input for the last step that jointly produces optimal estimates of camera poses and locations of 3D points. Such a pipeline has been implemented in several SfM software, such as COLMAP [20] and VisualSfM. We choose to implement our system based on COLMAP, since it offers improved robustness, accuracy, completeness and scalability, and has been released as an open-source software.

Regarding feature matching, there are several options, including exhaustive, sequential, spatial, and vocabulary-tree-based [21] feature matching. The exhaustive feature matching is slow, since each image must be compared with all the others. The sequential feature matching requires loop closure to prevent a large drift error. The spatial matching method requires spatial data like GPS as additional input, and often suffers from model fragmentation. Vocabulary-tree-based matching is a method where every image is matched against its visual nearest neighbours using a vocabulary-tree with spatial re-ranking which is recommended for large image collections. Since our system is supposed to work with a large amount of crowdsourced data such as unordered images, we select vocabulary-tree-based method which also proves to be more efficient and accurate than the others through our experiment.

The SfM pipeline outputs a 3D point cloud with random scale and orientation. Therefore, geo-registration is typically performed afterwards to re-scale and align the model with respect to the real world. The geo-registration function provided by COLMAP requires GPS coordinates of at least three locations on the data collection trajectories which are also uniformly spaced across the map. One way is to manually select three locations and obtain their GPS coordinators from Google Maps for example, and then transform the GPS coordinates into Cartesian coordinates. Another way is to enable positioning services such as real-time kinematic (RTK) during visual data collection.

COLMAP does not provide methods for change detection or automatic point cloud update. However, it provides functions of deleting certain images and their related 3D information. If any change in the scene has been detected and localized, it is possible to utilize these functions to delete the corresponding 3D points from the existing point cloud, and then register the images capturing the new scene into the point cloud. Therefore, the focus of this paper is placed on change detection and localization rather than the implementation of updating the point clouds.

Camera pose estimation. The output of the SfM pipeline contains the camera poses of each image successfully registered into the point cloud. After geo-registration, the camera poses are converted into world coordinates. The images which do not have enough common features with the others cannot be registered and would be dropped automatically during feature matching. Given a new image, its camera pose can be obtained by registering it into the point cloud. Compared with deep learning based camera pose estimation, such as PoseNet [10], obtaining camera poses from the SfM pipeline typically requires more computational costs but provides higher accuracy.

Semantic segmentation and object detection. are computer vision tasks that detect objects from an image and assign to them an appropriate class label. In case of semantic segmentation, a class label is assigned to each pixel in an

image, and multiple objects of the same class are not recognized as separate objects unless the instance segmentation is performed. Different than semantic segmentation, object detection provides an individual bounding box around every detected object. Our system combines both approaches, because object detection spots objects individually while semantic segmentation gives a more precise boundary around the detected object.

3 System Overview

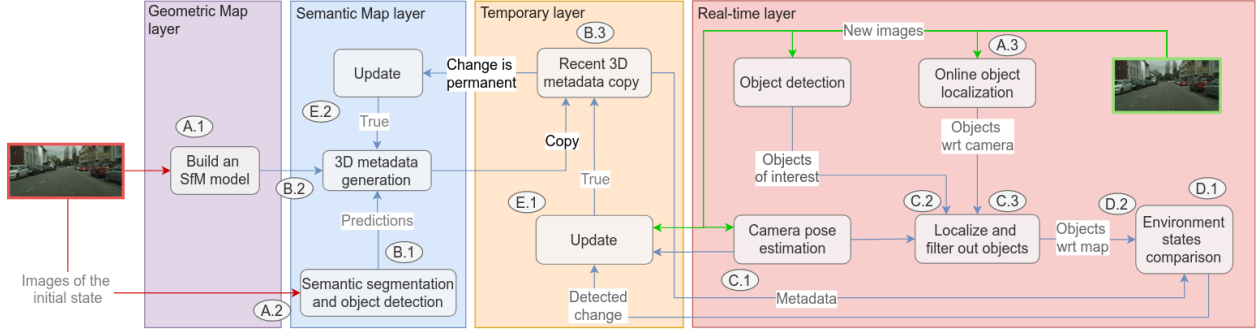


Figure 1: Architecture of a multi-layer map and the pipeline of creating and maintaining the map based on crowdsourced visual data.

We propose to create a four-layer map as illustrated in Figure 1. The first layer is the Geometric Map layer which stores the raw point-cloud and the predicted camera poses (trajectory) generated by the SfM. The second layer is a Semantic Map layer that stores the semantic information about static objects (e.g. types and locations of traffic signs) and the metadata (e.g. creation time) associated with the objects. Semantic information can be extracted from 3D point-cloud or directly from video/image data using computer vision techniques.

The next layer is the Temporary layer which contains the recent copy of the Semantic Map layer which is needed for temporary changes to avoid unnecessary remapping. For example, sometimes in work zones, underground pipes maintenance is performed, after which there are not always visual changes in the environment. Therefore, to not remap such a region, we need to store the work zone point-cloud in a separate layer, then, in case there are visual changes after the maintenance work is over, the permanent layer can be updated. Otherwise, the temporary data is discarded. The last layer is a Real-time layer where the change detection process is constantly repeating.

The map is created in two stages: the offline stage which creates static information for the geometric and semantic map layers, and the online stage which detects changes and extracts dynamic map information from crowdsourced visual data in real time.

Offline Stage. The first step is to build the initial SfM-based 3D model from video/images (refer to Step A.1). The resulted point clouds can be aligned with the existing 2D road maps such as Google Maps and OpenStreet Map. The information stored in the geometric map layer is valid typically for years.

The images used for creating the SfM model are utilized for detecting objects in the environment. Some deep learning networks have to be trained offline for a single time only unless the application or domain had been changed and require retraining. Those include camera pose estimation, semantic segmentation, object detection, and online object localization. For example, if an algorithm has been trained to classify traffic signs in one country, to work in another country - i.e. a new domain - it may need to be fine-tuned on a dataset with specific traffic signs of that country. The step indicated as A.2 is the image semantic segmentation and object detection - the two deep learning algorithms that are trained independently from each other. Step A.3 is the online object localization algorithm which predicts the 3D location as x , y and z of every pixel in an RGB image. This algorithm uses deep learning trained with labels obtained from SfM point-cloud at step A.1. The camera pose estimation at step A.3 requires SfM camera poses from step A.1 and must be trained offline as well.

The next step is 3D metadata generation. For this step, we first extract pixel-wise semantic segmentation predictions and bounding boxes from traffic sign detection at step B.1. Second, at step B.2, the point-cloud generated by the SfM at the initial step is segmented class-wise using the predictions from the semantic segmentation, this way generating the 3D metadata. The metadata is generated and stored in the Semantic Map layer. In the Temporary layer we store a recent copy of the metadata at step B.3. This copy is updated at step E.1 every time a change has been detected. If the change is classified as permanent, the original metadata is updated at step E.2 in the Semantic Map layer.

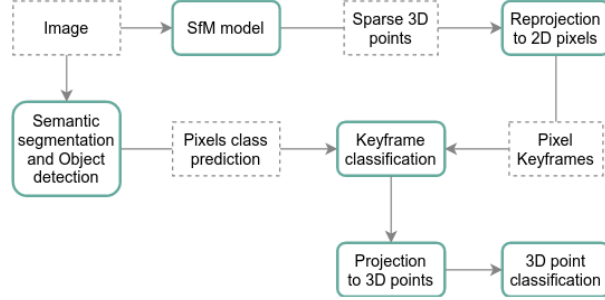


Figure 2: Workflow of semantic map layer generation.

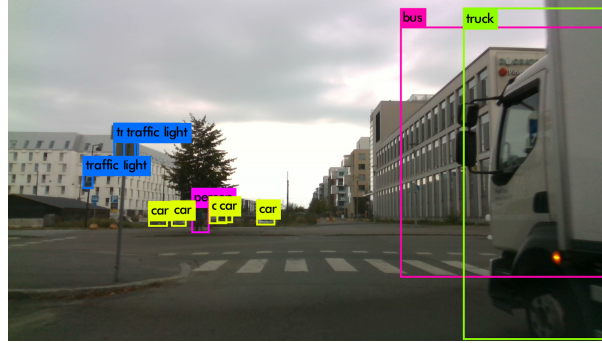


Figure 3: Example of object detection using YOLO

Online Stage. The next steps described are performed online in the Real-time layer. In order to continuously detect changes in the environment, at first it is necessary to localize the camera with respect to the 3D map/metadata at step C.1. The objects in the environment are localized at step C.3 and the classes of the objects are identified at step C.2. After the objects of interest are localized in 3D map, at step D.2, those localized objects are compared with the objects in the copy of the metadata at step D.1. The objects are compared according to the 3D position and the object classes. If the states differ, the change is reported to the cloud at step E.1, after which the images freshly collected in that region are sent to update the copy of the metadata. If the change was identified as temporary, the original metadata is not updated, while the copy of the metadata is discarded and a fresh copy is generated at step B.3.

In order to update the map efficiently, that is, to not have a mixed point-cloud from different environment states, the previous information of the map where the change was detected, including the 3D point-cloud and the metadata, must be deleted. That region should then be re-mapped with the freshly collected data after which the new metadata must be generated for that region. In the following subsections, we describe the methods for each step in more detail.

4 Semantic Map Layer

When the point-cloud is built, the next step is to generate the metadata, which is detailed information about the surrounding traffic environment. It defines objects of interest, such as traffic signs, road, and etc.

The semantic map data is represented as the metadata of the point-cloud. A group of 3D points associated with an object are tagged with the class of the object (e.g. traffic sign). In addition, the center of the group of points is tagged also with more detailed information of the object, such as the type of traffic sign and the duration of the construction work.

The detailed process of the metadata generation is demonstrated in Figure 2. The images from the initial state of the environment, that were used for the sparse point-cloud generation, are segmented using a semantic segmentation network by [17]. The output of the network represents a pixel-wise semantic prediction. The 3D points of the point-cloud are then semantically segmented according to the object classes of the 2D image keypoints that observe those 3D points. For example, if the image keypoint coordinates are x and y , then we assign that keypoint a class from the semantic segmentation at the coordinates x and y . Those image keypoints are accessed from the database of the model reconstructed by the SfM. The class of a 3D point is defined according to the confidence which is achieved by weighting all semantic segmentation predictions of the 2D image keypoints that observe the same 3D point. Each image keypoint that observes the same 3D point occupies a single pixel which has semantic segmentation probabilities for every class.

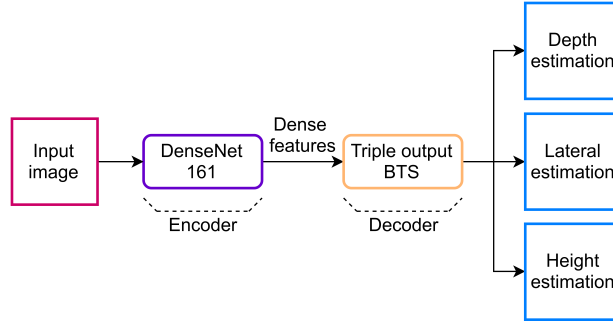


Figure 4: Network architecture of the online object localization algorithm.

The probabilities of every keypoint are averaged and the highest class probability is assigned to the 3D point. To classify the traffic signs the weights depend on the confidence of the YOLO [18] prediction.

The reasons for combining semantic segmentation with object detection are two-folded. Firstly, if the results of these two methods conflict, the results would be considered as invalid. To give an example, YOLO classified a truck in Figure 3 as a bus and a truck. If the semantic segmentation algorithm predicts it as a truck, the wrong prediction (i.e. bus) can be removed. Secondly, the bounding boxes surrounding the detected objects often contain lots of space and may cover some objects that belong to different classes. For example, in Figure 3, the building on the right side is partially covered by the bounding box associated with a truck. Since semantic segmentation provides pixel-wise prediction, by calculating the intersection of each bounding box and the corresponding segment, more precise boundaries of objects can be obtained.

5 Real-time and Temporary Layers

The collected video/images are processed online to detect potential changes in the environment and to update the semantic information accordingly. Besides object detection which is used also at the offline stage, we propose a deep learning based algorithm for online object localization.

Object localization. The algorithm predicts the position of an object in 3D space from an RGB image. At first, as shown in Figure 1, we use YOLO to detect traffic signs in the image. For every bounding box coordinates, we extract the pixel prediction of the bounding box centre from the localization prediction. After this step, we have multiple predictions per single traffic sign, since the same traffic sign might be observed in multiple images. At first, we filter out some noisy predictions using two parameters that have to be tuned: the minimum and the maximum distance from the camera to the detected point of a traffic sign. This step is helpful because the online localization algorithm tends to work better for closer distances. The next step is to combine the predictions by averaging the predicted locations within a specified radius parameter. This way we obtain the GPS locations of the traffic signs from an RGB image.

As the backbone for the convolutional neural network to train online localization algorithm, we use the BTS network for monocular depth estimation [11] which is shown in Figure 4. This is one of the best performing networks in the area at the moment, though, any other convolutional neural network would be possible to adapt for our method.

The model is initialized with the weights trained with Kitti depth dataset [7]. The output layer of the network is modified to produce a pixel-wise output with three channels for x, y, and z position of an object in 3D space. Originally it was producing a single channel pixel-wise depth prediction. To train the network, a specific dataset was generated, with a label for every image. More details about the dataset are described in Section 6.

For the three-channelled labels, we used the output of the previously reconstructed SfM model. The output of COLMAP [20] consists of multiple items, from which the estimated camera poses, the 2D image keypoints and positions of the 3D points projected from the 2D image keypoints were used.

The first channel of the label represents the x position of an image keypoint in 3D space with respect to the camera, and the other two channels represent y and z positions of the keypoint. To find these, the distances were calculated from the 3D points to the camera pose of the image. The 3D points are projected from the 2D keypoints of an image, which are limited, and are not available for every single pixel of the image. Therefore the remaining pixels, which do not contain any keypoints, are not considered when calculating the loss during training.

Metadata comparison After the metadata has been generated we compare it with the new state of the environment to detect changes as shown in Figure 1. At first, the camera is localized with respect to the current environment and the

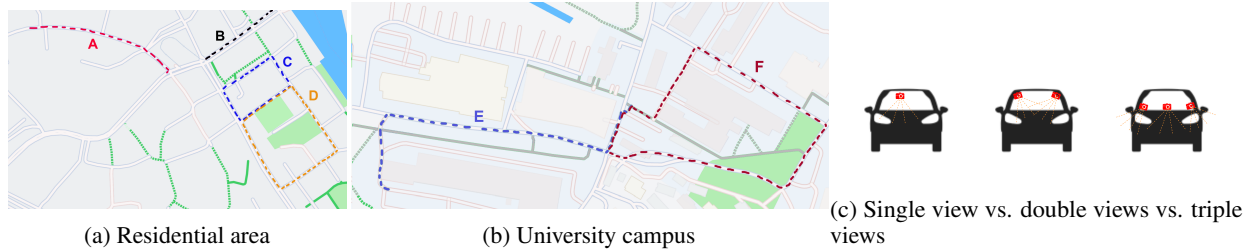


Figure 5: Data collection trajectories and camera placements.

3D metadata of the initial state. The traffic signs within a specified radius are detected, localized with respect to the environment and compared between the two states. If there is a mismatch then the change is reported and the temporary copy of the metadata is updated. The users, such as cars, can then give priority to the temporary layer information.

6 Datasets

We collected video data through cameras installed on vehicles from a university campus and a residential area on February 22, 2019 (Day 1) and December 2, 2019 (Day 2). We collected data along 2 trajectories in the campus, and 4 in the residential area. For data collection, we used Garmin 55 dashcam on Day 1 and Intel RealSense D435 on Day 2. The trajectories and camera setups are visualized in Figure 5. All the cameras were placed to face roughly the same direction, but were slightly rotated towards each other to have the camera views slightly overlapped.

The video resolution was set to 1920x1080, while the frame rate was 30 fps. The vehicles were running at a speed within the range between 20 and 30 km/h. Since the data was collected in different seasons, the scenes and the lighting conditions vary. For instance, we observed several changes of traffic signs from the data collected on Day 2.

The collected data, as summarized in Table 1, has been used for evaluating the performance of SfM-based point cloud generation, change detection, and object localization. Though all the video was collected at 30 FPS, a subset of the video was down sampled to 10 FPS before it is fed into the SfM pipeline. Datasets I-V include in total 12842 samples. When developing the online object localization algorithm, we divide all the samples into three subsets: 12086 samples for training, 50 samples for validation, and 706 for testing. To evaluate change detection, we used Dataset III and IV.

7 Evaluation of the Offline Processes

Our system generates the geometric map layer and the semantic map layer based on SfM reconstruction, semantic segmentation and object detection. The accuracy of semantic map data, particularly the classification and localization accuracy of traffic signs, is affected by the performance of the background technology in use. Therefore, we will evaluate the performance of each building block and analyze its impact on the overall accuracy of semantic map data.

We conducted all the experiments on a system running Ubuntu 18.04 and powered by four NVIDIA GTX 1080 Ti with 11GB of RAM each and two Intel Xeon Gold 6134 CPUs.

7.1 Geometric Map Layer

As discussed in Section 2, we implement 3D reconstruction based on COLMAP [20], and employ the vocabulary-tree-based method for feature matching [21]. For each trajectory described in Section 6, we create a sparse point cloud and perform geo-registration on the point cloud.

Table 1: Dataset description

Index	Date	Trajectory	Camera setup	FPS	# of images
I	Day 1	5b (E, F)	single view	10	460, 576
II	Day 1	5a (B)	single view	10	725
III	Day 1	5a (A)	double view	10	1525
IV	Day 2	5a (A)	single view	10	706
V	Day 1	5a (C, D)	triple view	30	945, 2874

We choose the data collected along Trajectory A (Dataset III) as example for detailed analysis. Figure 6 shows the camera poses obtained from the results of the SfM pipeline (i.e. each blue dotted line represents the poses of one camera) and the RTK samples (i.e. the red dotted line). The RTK samples were collected at 1Hz and were considered as ground truth. The estimated camera poses align with the RTK samples except the accumulated drift at the left end of the trajectory. Since the sampling rate of images is higher than that of RTK data, we calculate the error of camera pose estimation as the distance between each camera pose and its closest RTK sample. The average error is 2.329 meters for camera 1 and 2.238 meter for camera 2. Concerning the bias caused by different sampling rates, the actual errors may be lower than the ones we calculated.

For comparison, we retrained and tested PoseNet [10], a convolutional network for real-time 6-DOF camera relocalization, using our datasets. The median distance and orientation errors of PoseNet-based camera pose estimation are 6.2 meters and 3.4 degrees, respectively. As precise localization of objects like traffic signs relies on accurate camera pose estimation, the PoseNet-based solution cannot fulfill the accuracy requirement. To evaluate the other parts of the system, we use the camera poses produced by the SfM pipeline, leaving the improvement of PoseNet-like real-time camera relocalization for future work.



Figure 6: Estimated camera poses of Dataset III vs. RTK samples. Red: RTK, Blue: camera 1 and camera 2.

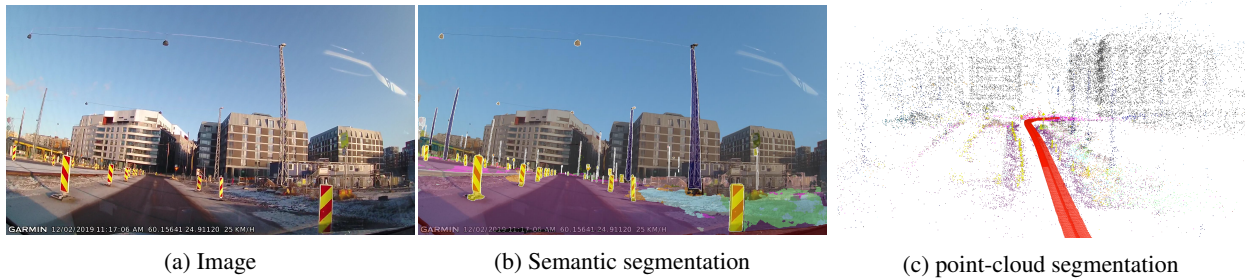


Figure 7: An example of semantic segmentation, point-cloud segmentation and object detection. At step 7a the image is semantically segmented and used for the step 7b to classify 3D points of such objects as buildings (grey), roads (purple), traffic signs (yellow), etc. The predicted by the SfM camera poses are shown with the red color in Figure 7c.

7.2 Semantic Map Layer

For each image registered in a point cloud, our system performs semantic segmentation and object detection to detect objects and 2D keypoints corresponding to each object. The results are then utilized for segmenting the point cloud and annotating 3D points with object classes.

Semantic segmentation. We implement semantic segmentation based on the Seamseg¹ architecture proposed by Mapillary [17]. The model trained and tested on the Mapillary dataset [13] achieves 50.4% IoU [17].

In the results of semantic segmentation, each segment is supposed to represent a certain class of object, such as building, lane, and traffic sign. By mapping the 2D image keypoints within each segment to the 3D points in the point cloud, the point cloud can be segmented by grouping the 3D points by the object classes of the corresponding 2D image keypoints. For example, the results of point cloud segmentation in Figure 7c are based on the results of semantic segmentation in Figure 7b. Note that the boundaries of objects must be precisely defined to reduce the error in the following object localization step. For example, if a segment that represents a traffic sign by accident covers part of a building from the background, the location of the traffic sign may be set to the location of the building, which is away from the ground truth.

¹<https://github.com/mapillary/seamseg>

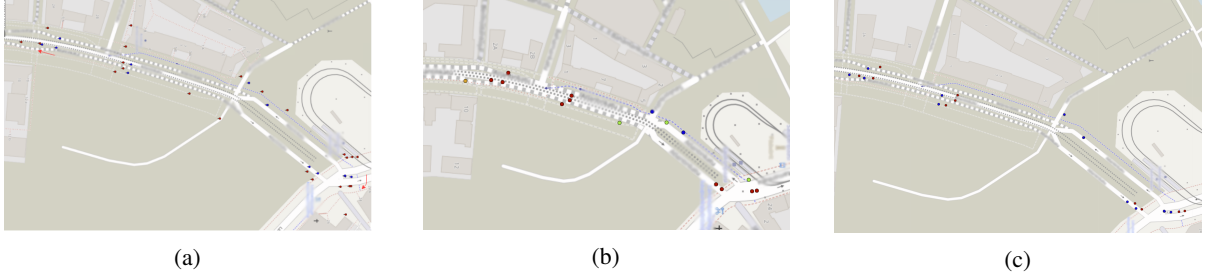


Figure 8: (8a) Locations of detected traffic signs with metadata generation: ground truth (red), predictions (blue); (8b) Online traffic sign localization: false positives (YOLO) - orange, false negatives (YOLO) - green, false negatives (tuning) - blue, detected correctly - red; (8c) Comparison of two object localization methods: metadata localization - blue, online localization - red

Object detection. For object detection we used the YOLO network² and trained it on Mapillary traffic sign dataset³. The Mapillary group does not release the test set. Therefore, the released validation set was split into a test set of 4165 images and a validation set of 1000 images. The quantitative performance of the YOLO algorithm [18] on Mapillary data achieves 29.72% mIoU (mean intersection over union) and 5.20% mAP at 50% IoU at 33000 iterations, which was selected by the best performance on the validation set.

The Mapillary dataset contains 100,000 images divided among 314 classes. This results in roughly 320 images per class. However, according to the guidelines provided by the creators of YOLO, for better performance, it is recommended to use at least 2000 different images for each class. This number is greatly above what is available for Mapillary. We attribute this reason to the low performance obtained.

To evaluate the design of object localization itself, we remove the results belonging to the classes of "other-sign" (a class corresponding to unidentified traffic signs) and "complementary-obstacle-delineator-g2" (traffic signs delineating boundaries between the road and non-drivable areas) to reduce the errors caused by inaccurate object detection. The first class was removed, since YOLO misclassifies random objects as other-sign. The second class was removed, because there were a lot more objects belonging to this class than any other classes in the testing areas. Such imbalanced data causes noisy YOLO predictions.

Object localization. To evaluate the accuracy of object localization, we choose Trajectory A as example and manually collected the ground truth of the 23 traffic signs (see Table 2 and Figure 8a) installed along the trajectory. Among these traffic signs, 7 (identified as classes 1, 3, 4, 6) were not recognized by YOLO as traffic signs, because they were not clearly visible in the images, and 4 (identified as classes 7, 4) were misclassified. As a result, 12 were detected and classified by YOLO correctly in at least one image frame. Among those 12 traffic signs, 3 (identified as classes 5, 1) were classified correctly but not localized. Object localization fails when there are insufficient 2D image feature keypoints that appear in the intersection between a segment and the corresponding bounding box of the object in question.

²<https://github.com/pjreddie/darknet>

³<https://www.mapillary.com/dataset/trafficsign>

Table 2: Traffic signs installed along Trajectory A on Day 1

Id	Class	Image	Count
1	information-pedestrians-crossing-g1		11
2	regulatory-keep-right-g1		3
3	regulatory-yield-g1		2
4	shared-path-pedestrians-and-bicycles-g1		2
5	regulatory-no-stopping-g1		1
6	information-parking-g5		1
7	warning-roadworks-g1		3

Table 3: Results of traffic sign localization. (a) - the number of clearly visible traffic signs, (b) - the number of traffic signs detected by YOLO, (c) - the number of traffic signs localized successfully, (d) - median error, (e) - standard deviation of the error

Total	(a)	(b)	(c)	(d)	(e)
23	16	12	10	7,72	5.16

Table 4: Depth, lateral and height errors of online 3D localization method at 670K training iterations

Set	Depth (m)	Lateral (m)	Height (m)
Validation	2.35	1.96	0.50
Test	6.06	8.036	0.708

As shown in Table 3, the median distance error of localized traffic signs compared with the ground truth is 7.72 meters with standard deviation of 5.16. The errors are mainly caused by the error in SfM-based 3D reconstruction and geo-registration. In our experiment, the data was collected from vehicles driving through the trajectories following one direction rather than two. We used up to 3 cameras facing to the front for data collection. More cameras facing different directions would be needed in order to reduce the error in depth prediction for the 3D points. The error in depth prediction causes error in point cloud segmentation. In addition, the GPS coordinates used for geo-registration were selected manually. The inaccurate GPS coordinates causes error in geo-registration. Due to that, some traffic signs which locate on the right side of a street were misplaced on the left side. Adjustment of geo-registration, such as re-scaling and rotation indicated with red arrows in Figure 8a, can significantly reduce the error in geo-registration.

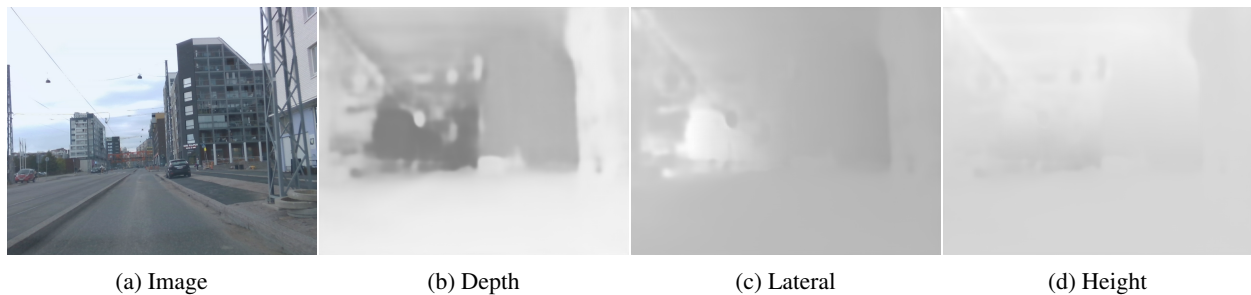


Figure 9: Predictions of online object localization from RGB at 80500 iterations

8 Evaluation of the Online Processes

For this method, we first detect traffic signs online using YOLO object detection and localize them in 3D map/metadata using the proposed online localization method. Then we compare the detected traffic signs with the information in the metadata to detect changes, as described in Section 5.

Online object localization. For 3D object localization we select BTS⁴ architecture as our baseline [11]. The performance of the network heavily depends on the accuracy of the training dataset, which is created from the SfM point-cloud, as described in Section 5. While the accuracy of the dataset depends on the following: the number of views with overlapping regions - with a larger number of views the point-cloud data are less noisy and the reconstruction is more accurate. Also, to improve the accuracy it can help to 1) train monocular neural network observing a scene from multiple perspectives for better generalization, 2) have a larger amount of reconstructed point-cloud data, by mapping larger area of the environment and by densifying the point-cloud 3) have an accurate geo-registration, since the scale of the SfM model directly affects the scale of the localization predictions in meters. For this reason, it is necessary to select GPS points as close as possible to the actual GPS of the camera poses.

This method assumes the camera pose to be predicted accurately for localization of the object’s global position. The model has been pre-trained on the Kitti dataset [7]. After that, the model has been trained for 670000 iterations with 1208 training samples from the dataset collected from 6 different regions of the environment.

Table 4 shows the results of online 3D localization on the validation set and on the test set. From these observations, it can be concluded that the lateral estimation from monocular data is the hardest task for the SfM and deep learning

⁴<https://github.com/cogaplex-bts/bts>

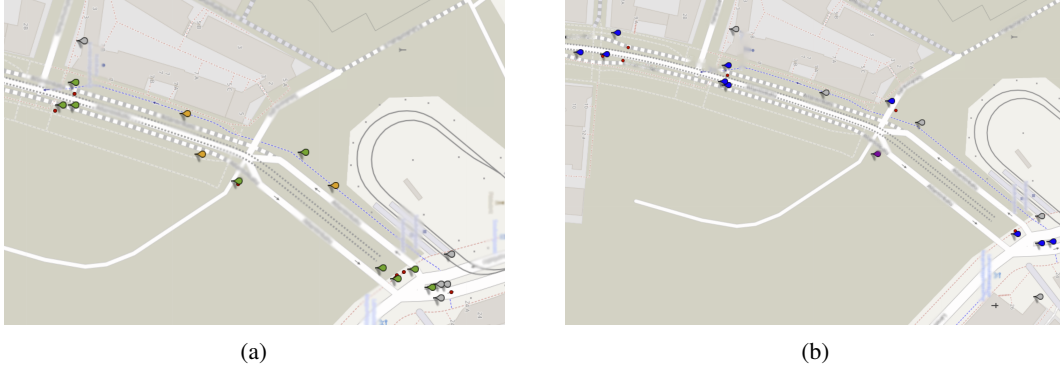


Figure 10: (a) Online localization on the new state of the environment. Ground truth: grey - hidden/hard to see traffic signs, yellow - misclassified by YOLO, green - classified by YOLO. Online localization: 7 red dots. (b) Change detection. Ground truth: grey - hidden/hard to see/unrecognizable by YOLO traffic signs, blue - expected to be localized. Online change detection method: 8 red dots - true positives, purple - false positive.

Table 5: Parameters for online localization (in meters). (a) the maximum distance from the camera to the detected point of a traffic sign which was predicted by the online localization algorithm, (b) the minimum distance and (c) the distance between points to be considered belonging to the same traffic sign.

State	a	b	c
Initial	21.5	10	10.5
New	21	0	11

among the three tasks. The qualitative results can be seen in Figure 9. Data augmentation such as color, gamma and brightness changes has been applied which helped to reduce overfitting but was not effective to reduce the error.

Online traffic sign localization in 3D map. In the previous subsection we evaluated the performance of the pixel-wise neural network with respect to the camera pose. In this experiment the task is to localize an object, specifically traffic signs, with respect to the 3D map, using the camera pose localization and the algorithm for online object localization from RGB data, which localizes objects with respect to the camera. The model we trained is overfitted to the dataset because we have limited data available for the training and the SfM reconstructions do not have the sufficient density. An example can be seen in Figure 9.

It has been observed that the algorithm works better for the cases when the camera is closer to the object. Especially the error is bigger for the depth and the lateral estimation. This might be happening due to the fact that when collecting the data for SfM reconstruction, when the object is farther, it is difficult to provide the algorithm with a variety of different viewpoints for a better localization, especially if the camera is moving towards the object. For better results the data must be collected in a way that the distant object can be observed from multiple viewpoints, therefore one camera could be moved forward while the other one laterally. Drone footage could be helpful as well.

There are three parameters that can be manually tuned for a better result (see Table 5). The remaining detected points, filtered out using the parameter tuning, are ignored. This tuning can be unnecessary if the online localization algorithm is trained with sufficient amount of SfM data.

One issue that has been encountered is that the YOLO model tends to work better for farther distances, while the online localization works better for closer distances. Therefore, it is challenging to tune the distance parameters. Sometimes important points might be filtered out. In this case, a solution would be to improve YOLO to work for closer distances and to provide predictions on more than a single frame.

In the first experiment, we test the algorithm using the same data from the initial state of the environment that was used for the initial metadata generation in order to compare the performance of both algorithms with respect to each other. After tuning the parameters for the tested region, one false positive (traffic sign) was detected due to YOLO misclassification as shown in Figure 8b, 4 false negatives due to YOLO misclassification, two false negatives due to the parameter tuning, since the traffic signs are located quite far from the camera, and 10 traffic signs were detected correctly. The results can be compared in Table 6.

With respect to the traffic signs localized by the metadata generation algorithm, the online localization missed one traffic sign as shown in Figure 8c. Also, it can be seen that the online localization algorithm is biased to localize the

Table 6: Online traffic sign localization tested on two states of the region: initial state and new state. (a) - clearly visible traffic signs, (b) - detected by YOLO algorithm, (c) - localized by the online localization method, (d) - average distance error with respect to the manually created ground truth (in meters), (e) - standard deviation of the error, (f) - median of the error

State	(a)	(b)	(c)	(d)	(e)	(f)
Initial	16	12	10	15.5	7.096	16.94
New	12	9	7	6.39	4.476	4.066



Figure 11: 11a, 11b Before and after visual-based change detection; Performance of Monodepth algorithm: 11c, 11d, 11e

objects as farther than the metadata generation algorithm (which is more reliable). For this reason, if needed, it is possible to perform a calibration to bring the online estimations closer to the metadata ones.

The next experiment tests the performance of online localization on the images from the new state of the environment (see Figure 10a and Table 6). The number of successfully localized traffic signs equals to 7/12, while the average error with respect to the ground truth equals to 6.39 meters. 3/5 were misclassified by the YOLO algorithm, while the remaining two due to the parameter tuning where the YOLO predictions are provided for the frames at farther distances.

The last experiment, described in the next subsection, demonstrates the performance of the change detection algorithm which is the performance of online localization with respect to the metadata of the old state of the environment.

Change detection and localization. In this section, we evaluate how accurately the online change detection algorithm can detect changes in traffic signs in terms of a quantity and the average distance error. We test the algorithm using two different states of the same map region. The threshold parameter is adjusted depending on the maximum distance error between the online localization and metadata localization to be considered as the same traffic sign but at different states of the environment. In this experiment, we set the threshold parameter to 17 meters. This means that two closest traffic signs from different states within 17 meters are considered to be the same object. If there isn't any traffic sign of the same type within 17 meters, then there is a change.

Table 7 shows how the algorithm performs with respect to the metadata and the ground truth. Assuming that the metadata contains accurate information, the algorithm identified 9 changes out of 9. The 3/9 new traffic signs have appeared in the current state of the environment and 6 traffic signs have been removed. The average error with respect to the ground truth is equal to 9.33 meters.

With respect to the manually labelled ground truth, considering only the traffic signs that are clearly visible in the images and only the ones which are recognizable by the YOLO network, the algorithm detects correctly 8 out of 10 traffic signs as shown in Figure 10b. The localization of the changes depends on the accuracy of the metadata and online localization methods. The false positive appeared due to mislocalization from the metadata generation side. One false negative is caused due to YOLO misclassification and the second one due to metadata parameter turning where the traffic sign was detected by YOLO while being too far from the camera.

9 Related work

In this section we review the latest works in the literature related to semantic mapping (metadata generation and maintenance) as well as change detection and localization.

3D mapping: Conventionally, 3D models for indoor and outdoor mapping are generated using laser scanners and depth cameras. In [5] 3D mapping is performed in the form of SLAM (Simultaneous localization and mapping) using the 3D laser range finder (LIDAR). Unlike SLAM which works with sequential data, SfM (Structure from Motion) allows 3D modeling using unstructured 2D image data which is more usable for crowd-sourcing applications. Agarwal et al. [1] reconstructed the regions of Rome city based on SfM using unorganized image data from internet photo-sharing sites.

Table 7: Results of change detection and localization. (a) - detected changes with respect to the metadata, (b) - detected changes with respect to the ground truth, (c) - false positives with respect to the ground truth, (d) - average error with respect to the ground truth (in meters), (e) - standard deviation of the error, (f) - median of the error

(a)	(b)	(c)	(d)	(e)	(f)
9/9	8/10	1	9.33	4.87	7.72

A more challenging task is to reconstruct large scale regions of cities rather than a single building. In [2] the large-scale dense reconstruction is performed using multi-view stereo approach on stereo image data. In this work we consider a possibility to use crowd-sourced data where there is no calibration information available. In [20] the reconstruction of a city includes the overhead view, while in urban driving way of crowd-sourcing this view is difficult to obtain. In this work we utilize the views from the front window on a car which is the most common in crowd-sourcing.

Metadata generation and maintenance:

In [16], the authors combined 2D image semantic segmentation with a LIDAR-based point-cloud to detect and localize in the 3D environment static landmarks such as roads, sidewalks, crosswalks and driveable area. After that, probabilistic methods were used to construct semantic HD maps comprised of multiple layers of metadata containing the landmarks. This method can be used to significantly reduce manual map creating efforts. The idea is similar to the proposed method for metadata generation in this paper, however we concentrate on SfM data to adapt for crowd-sourcing applications.

Semantic segmented images from RGB cameras were also fused with LIDAR point-clouds in [12] to build a semantic map for off-road autonomous driving. The generated maps contained metadata useful for spotting trails, obstacles, tall grass and leaf litter. The solution was then implemented in real-time on an off-road vehicle, which was able to safely traverse areas of rocky terrain and vegetation of various heights that were previously challenging for LIDAR-only systems.

Compared to our work, we opt for a cheaper to maintain solution, i.e. point-cloud created and updated using SfM [14] and RGB images. Our work includes temporary information management and we focus on traffic signs for metadata generation and apply this to an under-explored scenario: change detection.

Change detection and localization:

Gehring *et al.* [6] propose a voxel-based mobile laser scanner approach for change detection in a large scale urban environment. [19] proposes a change detection method based on LIDAR data. The extract clusters from pointclouds and assess the temporal behavior of those. In this work we concentrate on change detection using SfM pointcloud data which allows reliable change detection and localization using image data.

In [15], the authors developed an approach for spotting differences between an existing 3D model of an environment and a small sequence of images recorded in the environment. An image of the sequence is first projected onto the 3D model and then back to the view-point of another image of the sequence. Then, their method works by finding inconsistencies between such back-projected and real image pairs. It is, however, required that the locations of all images with respect to the 3D model are precisely known - which might require GPS, IMU and visual odometry. The proposed method does not provide state-of-the-art results, however, as the authors claim, the strong point of the method is that it is substantially fast to be executed on a mobile robot. Since their approach was only evaluated for small point-clouds, it is unknown if it is scalable to complex urban environments that can occupy very large areas. Furthermore, it requires the use of dense point-clouds, which may be challenging to generate with images from limited viewing angles and taken from a moving vehicle.

Alcantarilla *et al.* [3] developed a change detection system for urban scenarios. First, their approach consisted in obtaining two dense 3D reconstructions, each representing states of the environment at different times. After that, an accurate geo-registration on both point-clouds was performed, which allowed the alignment of both models. This alignment was used to obtain pairs of images (each image from a different state of the environment) taken at the same location. For each pair of images, a dense convolution neural network - trained via supervision - was employed to detect changes. Their method proved effective in detecting changes under different lighting and seasonal conditions. Again, the limitation of the method is the requirement for 3D dense reconstructions of both states. Also this method can only work as an offline solution.

We have tested a monocular change detection network SceneChangeDet⁵ [9]. An example of the before and the after image is shown in Figure 11c. The two images are almost perfectly aligned, which in practice is not easy to perform, especially with crowd-sourcing. In this example, the approximate locations of the two changes, which are two cars,

⁵<https://github.com/gmayday1997/SceneChangeDet>

were identified. However, in a more complex scene, when there are dramatic changes, like in the region where we test our methods, the visual-based method fails at detecting changes.

All these change detection methods address the task of change detection but localization is neglected. In our work we address the problem of change localization in the 3D map. Lee *et al.* [11] designed a neural network architecture based on the encoder-decoder scheme to perform depth estimation from monocular images. In their architecture, based on the locally planar assumption, the authors proposed a novel layer - named local planar guidance (LPG) - located in the decoder block of the network. The experiments have shown that their method outperforms previous ones with a significant margin in diverse metrics, providing state of the art results.

Monodepth2 method [8] estimates depth from a sequence of RGB images. It is a self-supervised training method which makes it possible to fine-tune it without a labeled dataset. The performance of the model trained on Kitti dataset [7] was unsatisfactory since the boundaries of estimated depth were blurred (see Figure 11d). The performance after training the model on our data has not demonstrated satisfactory results either (see Figure 11e). The limitation of monocular depth estimation methods is that they do not provide the 3D localization such as height and lateral information. We propose an end-to-end 3D localization network to solve this problem.

10 Discussion

A challenging task is to detect a change in case if a traffic sign has been shifted from one side of the road to the other. The algorithm will not be effective at detecting changes if the traffic sign is facing the same direction and is shifted within the distance indicated for the threshold parameter. For this reason, the road boundaries and markings should be specified in the metadata as well.

For future work, we plan to improve the accuracy of object detection and geo-registration, and to evaluate the system in different urban environments with more diverse changes. We plan to test the system for indoor applications. Another future direction would be to combine the method with other layers containing LIDAR data to improve accuracy.

11 Conclusions

In this paper, we presented a system for creating and updating a multi-layer HD map for autonomous driving.

Our system is partially built on top of other existing methods, e.g., SfM, semantic segmentation and object detection. Nonetheless, the system brings new functionalities and addressed a number of challenges to enable online change detection in rapidly changing urban environments. The system utilizes crowdsourced image and video data to build and update the 3D maps and the metadata and to detect and localize changes in real-time. Our solution could spot 80% of changes in the environment and localize them within roughly 9 meters precision.

References

- [1] S. Agarwal, Y. Furukawa, N. Snavely, I. Simon, B. Curless, S. M. Seitz, and R. Szeliski. Building rome in a day. *Communications of the ACM*, 54(10):105–112, 2011.
- [2] P. F. Alcantarilla, C. Beall, and F. Dellaert. Large-scale dense 3d reconstruction from stereo imagery. Georgia Institute of Technology, 2013.
- [3] P. F. Alcantarilla, S. Stent, G. Ros, R. Arroyo, and R. Gherardi. Street-view change detection with deconvolutional networks. *Autonomous Robots*, 42(7):1301–1322, 2018.
- [4] J. Dong, M. Noreikis, Y. Xiao, and A. Ylä-Jääski. Vinav: A vision-based indoor navigation system for smartphones. *IEEE Transactions on Mobile Computing*, 18(6):1461–1475, 2019.
- [5] D. Droschel, M. Schwarz, and S. Behnke. Continuous mapping and localization for autonomous navigation in rough terrain using a 3d laser scanner. *Robotics and Autonomous Systems*, 88:104–115, 2017.
- [6] J. Gehring, M. Hebel, M. Arens, and U. Stilla. A voxel-based metadata structure for change detection in point clouds of large-scale urban areas. *ISPRS Annals of Photogrammetry, Remote Sensing & Spatial Information Sciences*, 4(2), 2018.
- [7] A. Geiger, P. Lenz, and R. Urtasun. Are we ready for autonomous driving? the kitti vision benchmark suite. In *2012 IEEE Conference on Computer Vision and Pattern Recognition*, pages 3354–3361. IEEE, 2012.
- [8] C. Godard, O. Mac Aodha, M. Firman, and G. J. Brostow. Digging into self-supervised monocular depth prediction. October 2019.

-
- [9] E. Guo, X. Fu, J. Zhu, M. Deng, Y. Liu, Q. Zhu, and H. Li. Learning to measure change: fully convolutional siamese metric networks for scene change detection. *arXiv preprint arXiv:1810.09111*, 2018.
 - [10] A. Kendall, M. Grimes, and R. Cipolla. PoseNet: A convolutional network for real-time 6-dof camera relocalization. In *Proceedings of the IEEE international conference on computer vision*, pages 2938–2946, 2015.
 - [11] J. H. Lee, M.-K. Han, D. W. Ko, and I. H. Suh. From big to small: Multi-scale local planar guidance for monocular depth estimation. *arXiv preprint arXiv:1907.10326*, 2019.
 - [12] D. Maturana, P.-W. Chou, M. Uenoyama, and S. Scherer. Real-time semantic mapping for autonomous off-road navigation. In *Field and Service Robotics*, pages 335–350. Springer, 2018.
 - [13] G. Neuhold, T. Ollmann, S. Rota Bulò, and P. Kotschieder. The mapillary vistas dataset for semantic understanding of street scenes. In *International Conference on Computer Vision (ICCV)*, 2017.
 - [14] O. Ozyesil, V. Voroninski, R. Basri, and A. Singer. A survey of structure from motion. *arXiv preprint arXiv:1701.08493*, 2017.
 - [15] E. Palazzolo and C. Stachniss. Fast image-based geometric change detection given a 3d model. In *Proceedings of the IEEE Int. Conf. on Robotics & Automation (ICRA)*, 2018.
 - [16] D. Paz, H. Zhang, Q. Li, H. Xiang, and H. Christensen. Probabilistic semantic mapping for urban autonomous driving applications. *arXiv preprint arXiv:2006.04894*, 2020.
 - [17] L. Porzi, S. Rota Bulò, A. Colovic, and P. Kotschieder. Seamless scene segmentation. In *The IEEE Conference on Computer Vision and Pattern Recognition (CVPR)*, June 2019.
 - [18] J. Redmon, S. Divvala, R. Girshick, and A. Farhadi. You only look once: Unified, real-time object detection. In *Proceedings of the IEEE conference on computer vision and pattern recognition*, pages 779–788, 2016.
 - [19] J. Schachtschneider, A. Schlichting, and C. Brenner. Assessing temporal behavior in lidar point clouds of urban environments. *International Archives of the Photogrammetry, Remote Sensing and Spatial Information Sciences-ISPRS Archives 42 (2017), Nr. 1W1*, 42(1W1):543–550, 2017.
 - [20] J. L. Schönberger and J.-M. Frahm. Structure-from-motion revisited. In *Conference on Computer Vision and Pattern Recognition (CVPR)*, 2016.
 - [21] J. L. Schönberger, T. Price, T. Sattler, J.-M. Frahm, and M. Pollefeys. A vote-and-verify strategy for fast spatial verification in image retrieval. In *Asian Conference on Computer Vision*, pages 321–337. Springer, 2016.